

A Plasma-Generating N-95 Respirator Decontamination Unit Created from a Microwave Oven

David N. Ruzic,* Chamteut Oh, Joseph V. Puthussery, Dhruval Patel, Zachary Jeckell, Vishal Verma, & Thanh H. Nguyen

University of Illinois, Urbana IL, 61801, USA

*Address all correspondence to: David N. Ruzic, University of Illinois, Urbana IL, 61801, USA; Tel.: 217-840-3282, E-mail: druzic@illinois.edu

ABSTRACT: Wearing a mask population-wide is an important preventive measure in addressing COVID-19 and potential future pandemics. We showed how a household microwave oven, a coat-hanger, and a coffee cup can generate plasma that can be used to decontaminate N95 respirators in less than 1 minute. We proved that microwave-generated plasma can reduce infectivity of the Tulane virus and the transmissible gastroenteritis virus (TGEV) on N95 respirators by $> 3\text{-log}_{10}$. We further studied the Tulane virus by molecular assays to understand inactivation mechanisms, and we found that the plasma damages both viral proteins and genomes. Spectroscopy of the plasma revealed OH and C-containing radicals as the most prevalent active species expected to cause virus inactivation. The respirators still maintained filtration and fit even after 10 cycles of the plasma treatment. We believe that microwave-generated plasma is an easily accessible respirator decontamination technique that everyone could use for safe respirator reuse.

KEY WORDS: COVID-19, N-95 respirator, decontamination, plasma, microwaves

I. INTRODUCTION

The COVID-19 pandemic has caused unprecedented impacts on public health and the global economy.^{1,2} SARS-CoV-2 features higher transmissibility than other coronavirus epidemics (such as SARS and MERS) and higher mortality than the pandemic influenza.³ More important, epidemiological studies report that asymptomatic or minimally symptomatic patients also spread the virus efficiently.^{4,5} An increasing amount of scientific evidence proves that wearing a mask population-wide helps to curb transmission of virulent viruses.^{6,7} Although several types of vaccines proven safe and effective through phase III clinical trials are now available, wearing a mask is still considered a necessary preventive measure because achievement of herd immunity takes time, especially for countries that are left behind for vaccine supply.⁸ In addition, emerging variants of SARS-CoV-2 could show a higher reproduction rate (R_0) due to higher transmissibility than the wild type, so a higher percentage of the population may need to be vaccinated to reach herd immunity.⁹ For example, a delta variant (B.1.617.2), which became the dominant strain in the UK, caused a surge of confirmed patients but 62% of the population had their first jab and 44% are fully vaccinated as of June 2021.¹⁰

With scientific support and a positive perception of mask wearing, demand for respirators will remain high throughout the current pandemic and surge again in future pandemics.¹¹ Depletion of respirators did not happen for the first time in the current pandemic; rather, there were respirator shortages back in 2004 (SARS) and 2009 (H1N1).¹² To address the respirator shortage, the Center for Disease Control and Prevention (CDC) and the Food and Drug Administration (FDA) temporarily recommended reuse of respirators with the requirement of decontamination efficacy ($> 3\text{-log}_{10}$ infectivity reduction), keeping filtration efficacy, leaving no toxic materials for users.^{13,14} Different decontamination technologies have been suggested and evaluated in terms of the above mentioned requirements. For example, Schwartz et al. (2020)¹⁵ demonstrated that a commercial device generating hydrogen peroxide vapor could successfully inactivate 6-log_{10} *Geobacillus stearothermophilus* spores at a large scale. Yang et al.¹⁶ summarized cases where ultraviolet germicidal irradiation (UVGI) successfully inactivated influenza viruses harbored on respirators. Lee et al.¹⁷ invented a dielectric barrier discharge plasma generator to produce ozone gas, which reduced 4-log_{10} infectivity of human coronavirus (HCoV-229E) on respirators. However, most of these technologies require special instruments or devices that ordinary people cannot easily access, and this is a critical issue that limits respirator reuse population-wide. Although the CDC suggested that respirators can be kept inside breathable paper bags for at least five days to reduce SARS-CoV-2 infectivity,^{18,19} healthcare workers and others are left to choose either effective but less accessible or accessible but less effective options.

Plasma has been studied for pathogen inactivation for decades.²⁰ Although its chemistry is tunable by optimizing carrier gas, plasma normally consists of various reactive nitrogen/oxygen species and UV,²¹ whose diversity enables inactivation of a wide range of pathogens (i.e., bacteria, fungi, and virus).²² In addition, plasma inactivation is known to be nondestructive, and this feature makes plasma applicable to the biomedical and food industries, where conventional disinfectants are limited due to toxicity and destructive reactions.^{23,24} Commercial plasma sterilization devices are not widely available and are costly, so only a few if any hospitals, nursing homes, or other medical facilities are expected to have them. However, plasma is widely known to be created by irradiating grape hemispheres in a household microwave oven, which people can easily access.²⁵ Our previous study succeeded in controlling and applying the plasma generated by a 2.45-GHz microwave oven in ambient air to engineering purposes.²⁶

The goal of this study was to turn a household microwave oven into a plasma-generating unit for respirator reuse. This decontamination unit only requires a household microwave, coffee cups, a coat-hanger, saline, and 3% hydrogen peroxide, all of which are easily available. We applied this unit to a N95 respirator contaminated by each of two viral species (Tulane virus and porcine coronavirus) and evaluated virus inactivation efficacy and respirator performance (filtration efficiency and fit tests). We confirmed that the microwave-generated plasma decontaminated the respirator without compromising its performance. The ability to turn a microwave oven into a decontamination device with common materials means instant worldwide accessibility. We believe this will contribute to addressing respirator depletion in current and potential future pandemics.

II. METHODS

A. Microwave-Generated Plasma

The new idea described in this work is to create a plasma by making an antenna that has a length equal to some multiples of the wavelength of 2.45-GHz microwaves in a microwave oven (some multiple of 12.2 cm) and bending it into a split ring with a small (2-mm) gap. An intense electric field is generated in the gap that can ignite plasma under the right conditions. Those conditions are created by adding a conducting liquid, such as saline solution, into the gap and placing the antenna cap on a piece of ceramic. The conducting fluid electrically shorts the gap, causing a large current to flow and heat the fluid quickly. The water is vaporized in a few seconds and a spark is generated in the gap (Fig. 1). These first electrons then allow the plasma to be generated in the gap out of the materials present. The plasma is sustained as long as the microwave power is present. The plasma generates UV light and radicals, particularly carbon-containing

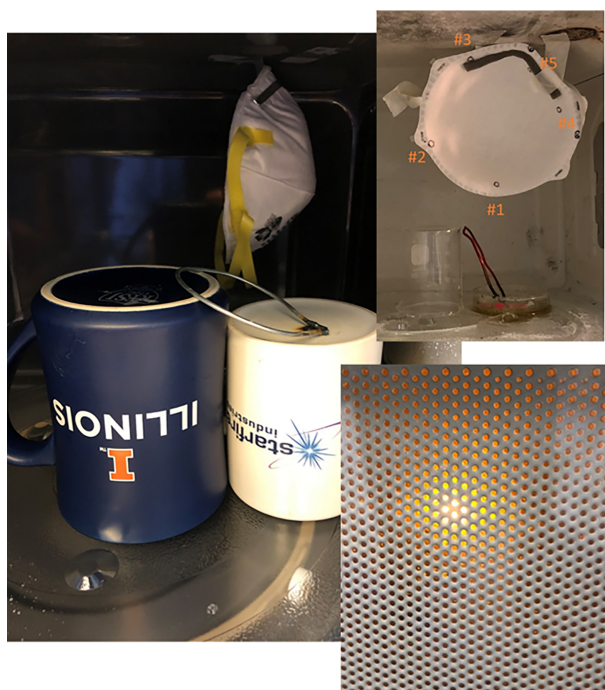


FIG. 1: Antenna on inverted coffee cup in microwave oven with N-95 respirator suspended behind it. (Bottom inset): intense plasma created at the antenna gap on the cup surface. The plasma could cause soot on materials near the plasma source. However, we found no microwave malfunction after more than 100 cycles. The intact respirator or pieces of respirator were put on the upper surface of the microwave throughout the experiments. Thus, inactivation efficacy may differ if the respirator is placed differently.

radicals from the ceramic surface. Hydrogen peroxide (at both 3% and 30%) added to the gap with the saline produces hydrogen peroxide vapor and OH radicals. Positive and negative ions and electrons are generated as well. All of these species are potential disinfectants for virus inactivation in this study.^{23,24}

The procedure to produce the plasma is as follows:

- First, obtain a piece of heavy-gauge (8–12) wire that is stripped of insulation, such as a metal coat-hanger. Cut it to 24.4 cm. Bend it into a circle leaving a gap of around 2 mm. This produces a split-ring antenna with a length of 2 times the wavelength of the 2.45-GHz microwaves which power microwave ovens. Through experimentation, we learned that the length must be within 5% (i.e., 24–25 cm). The gap must be between 1 and 2.5 mm.
- Second, disable the rotating arms in the microwave oven simply by turning the turntable dish upside down.
- Third, place the antenna with the gap down into glass or ceramic such as a coffee cup. Both ends of the antenna forming the gap should be touching the ceramic/glass surface. The antenna may need to be tilted up and supported to achieve this (Fig. 1).
- Fourth, add some saline solution (around 1 mL) and some normal household 3% hydrogen peroxide (at least 1 mL) to the antenna gap. If you do not add a conductive fluid, you will not be able to initiate plasma.
- Fifth, turn the microwave up to its highest power (i.e., normal operation) for 1 minute maximum. At first the liquid will start boiling. In about 15 seconds a popping sound and bright sparks will emanate from the gap (Fig. 1, bottom inset). Soon, continuous plasma will form, and a loud buzzing sound will be heard. The continuous plasma should run for at least 30 seconds. Note that to prevent the respirator from being damaged, it should not be left in for more than 1 minute. We published a how-to video showing the complete process and including safety tips.²⁷
- Sixth, wait for 5 minutes to cool down the antenna or metals in the respirator.

B. Virus Inactivation Experiments

We used two viral species, Tulane virus and transmissible gastroenteritis virus (TGEV), to evaluate the inactivation efficacy of our device. Tulane virus is in the *Calicivirus* family and is a surrogate for human norovirus. It is a nonenveloped virus with a single-stranded RNA within the same Baltimore classification as SARS-CoV-2. The FDA's guideline for respirator decontamination requires $> 3\text{-log}_{10}$ infectivity reduction of a nonenveloped virus, which is considered more resistant than enveloped viruses in general.¹⁴ Tulane virus was received from the Cincinnati Children's Hospital Medical Center. MA104 cells were purchased from ATCC (CRL-2378.1) and used as the host cells for the virus as described elsewhere.^{28,29} The complete medium for the MA104 cells was a mixture of 1X minimum essential medium (MEM; Thermo Fisher Scientific) with 10% fetal bovine serum (FBS; Thermo Fisher Scientific), 1X antibiotic-antimycotic (Thermo Fisher Scientific), 17 mM

of NaHCO_3 , 10 mM of HEPES, and 1 mM of sodium pyruvate. The virus was inoculated to the MA104 cells with 90% confluency and incubated at 37°C with 5% CO_2 for 3 days in order to multiply the virus particles. The viruses were harvested by three cycles of freezing and thawing and then purified by centrifugation (Sorvall Legend RT Plus, Thermo Fisher Scientific) at 2,000 rpm (556 g) for 10 minutes, filtered through a 0.45- μm filter (Millipore Sigma), and ultracentrifuged (Optima XPN-90, Beckman Coulter) at 1,000 rpm (116 g) for 5 minutes followed by 36,000 rpm (150,700 g) at 4°C for 3 hours. The virus pellets on the ultracentrifuge tubes were suspended in 1X PBS and kept at -80°C until use. The final virus concentration was about 10^7 PFU/mL.

TGEV is a porcine coronavirus belonging to the *Coronaviridae* family. It shares similar structural characteristics with SARS-CoV-2. For example, TGEV has a membrane encapsulating the nucleocapsids. Its positive single-stranded RNA genome is about 28 kb long. TGEV was provided by the Veterinary Diagnostic Laboratory at the University of Illinois at Urbana-Champaign. ST cells obtained from ATCC (CRL-1746) were used as the host cells. The ST cells were supplemented by the same complete medium described for the MA104 cells. TGEV was inoculated to the ST cells and incubated for 5 days at 37°C with 5% CO_2 . It was then harvested by three cycles of freezing and thawing. The large impurities from the cell debris were removed by centrifuge and filtration, which were used for purification. The final TGEV concentration was about 10^6 PFU/mL.

Artificial saliva was prepared by mixing six major compositions listed in ASTM E2700-16 in distilled water (Table 1). Each virus solution was mixed with the artificial saliva at a ratio of 1:1 to mimic where the virus is shed from the patient's mouth.³⁰ A droplet of the testing solution was inoculated to respirators with a pipette. The inoculated respirator was left inside the biosafety cabinet until the solution was thoroughly evaporated (about an hour). The temperature and relative humidity inside the biosafety cabinet were maintained at about 20°C and 30%–50% throughout the experiments (A600FC, General Tools). The testing solution was inoculated to either a whole respirator or small pieces of respirators depending on the purpose. First, the testing solution was seeded to five places inside and five places outside of the N95 respirator (Fig. 1, top inset) to check the impact of respirator shape on inactivation efficacy. The contaminated respirator was placed above the antenna inside the microwave oven as shown in Fig. 1. Both sides of

TABLE 1: Composition of artificial saliva

Reagent	Amount
$\text{CaCl}_2 \cdot \text{H}_2\text{O}$	0.13 g
NaHCO_3	0.42 g
NH_4Cl	0.11 g
NaCl	0.88 g
KCl	1.04 g
(Porcine gastric) mucin	3.00 g
Water	1,000 mL

the respirator were in direct line-of-sight with the top of the coffee cup. The microwave oven was then turned on for 30 s with 30% hydrogen peroxide and the antenna. The testing solution was inoculated to rectangular pieces of respirator [width:length = 15:5 (mm) measured from the top view] to determine inactivation efficacy under different inactivation methods but the same location. The pieces of respirator were put in the microwave oven and exposed to the microwave for 1 minute alone (without saline, hydrogen peroxide, or the antenna), then the microwave for 1 minute with saline only, the microwave for 1 minutes with saline and 30% hydrogen peroxide for the first set of experiments and the microwave for 40 seconds with saline and 3% hydrogen peroxide for the second set of experiments; finally, the microwave for 40 s with all the components (either 30% or 3% H₂O₂) including the antenna. As mentioned in the introduction, it takes at least 10 seconds to initiate plasma. That is why the comparison tests without plasma but with microwave energy were conducted for at least 40 seconds. All of the experiments were intended to determine its role in inactivating viruses. After the decontamination process, each inoculation site on the intact respirator was cut into 10-mm-diameter pieces. The pieces were submerged in 1 mL of culture medium without FBS. The viruses were then detached from the respirator pieces by vortexing them for 3 minutes and shaking them for 30 minutes at 450 rpm. The infectious virus concentration in the inoculum and the washing solution was about 10^{6.5} and 10⁶ PFU/mL, respectively, showing around 30% virus detachment efficiency over the viral infectivity ranging from 10^{2.2} to 10^{5.4} PFU per respirator piece. The same procedure was carried out with the negative controls which had been left in the biosafety cabinet throughout the experiments (about an hour).

The detached virus solutions were analyzed for the effects of treatment. The infectivities of the Tulane virus and TEGV were determined by plaque assay.³⁰ The host cells were prepared in 6-well plates two days before the inactivation experiments. The 10-fold serial dilutions of virus solution were prepared and 700 µL of each dilution was inoculated to each well with its host cells. The viruses on the cell monolayer were incubated at 37°C with 5% CO₂. The plates were gently shaken every 15 minutes to facilitate virus attachment to the cells. After 1 hour of incubation, the virus solution was aspirated and 2 mL of overlay solution was put into the well. The overlay solution contained 1.31 mL of 2X MEM, 0.5 mL of 1% agarose solution, 0.1 mL of FBS, 0.05 mL of 15-mM HEPES, 0.03 mL of 7.5% sodium bicarbonate, and 0.01 mL of 100X antibiotic-antimycotic. The overlay solution was solidified at 4°C and incubated further until plaque formation, which came at 2 days for Tulane and TGEV. After incubation, the cells were fixed on the wells using 10% formaldehyde for 1 hour. Then the plaques were visualized with 0.05% crystal violet in 10% ethanol for 20 minutes.

The Tulane virus was further studied by molecular assays to understand inactivation mechanisms. We used three molecular assays: two-step RT-qPCR, RNase, and binding. Each assay was designed to track damages on the genome, capsid proteins, and receptor-binding proteins, which are the main viral components. The two-step RT-qPCR consisted of two PCR steps:¹⁰ cDNA synthesis covering 80% of the Tulane virus genome and qPCR quantifying the cDNA. This assay assumed that any damage on the viral genome, which are a template for cDNA synthesis, would prevent the cDNA synthesis which ends up not

being quantified at the qPCR step. The genome was extracted from the samples using a QIAmp Viral RNA Mini Kit (Qiagen). The cDNA (5,534 bp long) synthesized from the extracted genome using the thermal cycler (MyCycler, Bio-Rad) and the ProtoScript First Strand cDNA Synthesis Kit (New England BioLabs). Finally, the cDNA was quantified by qPCR (QuantStudio 3, Thermo Fisher Scientific) and PowerUp SYBR Green Master Mix (Applied Biosystems). We followed the recipes for genome extraction, cDNA synthesis, and qPCR provided by the manufacturer. Information on primers and thermocycles are provided in Table 2.³⁰ The RNase assay used RNase (A/T1 mix, Thermo Fisher Scientific), an enzyme-degrading RNA, and RNase inhibitors (SuperRNase Sigma Aldrich) to quench RNase activity. The virus sample was incubated with the RNase at 37°C for 30 minutes, the RNase inhibitor was then incubated at 37°C for 30 minutes. This assay hypothesized that if the capsid proteins are damaged (more than 3.8 nm), the RNase can penetrate the viral shield and degrade the genome.³¹ After the RNase assay, the number of genomes was quantified by two-step RT-qPCR. The binding assay uses porcine gastric mucin conjugated with magnetic beads (PGM-MBs) to attract viruses with intact receptor-binding proteins.^{28,32} The mixture of 10 μ L of virus solution, 10 μ L of beads, and 980 μ L of PBS was gently shaken for 30 minutes. We assumed that only viruses with intact binding ability would bind to the PGM-MBs. The supernatant was aspirated while the virus-containing beads were being held on the tube by the magnet. The beads were rinsed with 1X PBS by vortexing the solution, and the supernatant was removed to get rid of the unbound viruses. This washing process was repeated three times. Then the genome on the beads was extracted using the QIAmp Viral RNA Mini Kit. The number of genomes was quantified by qPCR (QuantStudio 3, Thermo Fisher Scientific) and iTaq Universal SYBR green reaction mix (Bio-Rad Laboratories). The qPCR cocktail consisted of 3 μ L of RNA, 0.3 μ L of 10- μ M TV-NSP1-qPCR-F primer, 0.3 μ L of 10- μ M TV-NSP1-qPCR-R primer, and 1.275 μ L of nuclease-free water. Detailed information on one-step RT-qPCR is provided in Table 2. We applied the three molecular assays (two-step RT-qPCR, RNase, and binding) to both the plasma-treated samples and the negative controls. The data for the plasma-treated samples were normalized on a log-scale to that of the negative controls (i.e., $\log C/C_0$) to describe the integrity change in the viral structures by the plasma treatment.

C. Illinois Filtration and Fit Testing

Circular sections cut from one test respirator (2 circular sections of 47-mm diameter) were loaded onto a filter holder (URG,) and exposed to dried and charge-neutralized polydisperse 2% NaCl aerosols generated using a constant output atomizer (TSI Model 3076). The face velocity on the filter was maintained at 9.4 cm/s, which is equivalent to an effective flow rate of 85 Lpm (the NIOSH-recommended most severe breathing flow rate) through the entire respirator area [the surface area of the respirator was measured manually (~ 150 sq. cm)]. NaCl particle number concentration was measured before and after connecting the test filter using a condensation particle counter (CPC; TSI Model 3022A with a flow rate = 1.5 Lpm). The particle filtration efficiency of the tested filter material was calculated as

TABLE 2: RT-qPCR conditions and primers³⁰

Assay	Process	Primer name	Sequence (5'–3')	Position in genome	Amplicon length (bp)	Reaction condition
Two-step RT-qPCR	cDNA synthesis	TV-VP2-R	AGCGAGAGAAAA GCCTGCA	6213–6232	5,354	42°C for 60 min; 80°C for 5 min
	qPCR	TV-NSP1-qPCR-F	GTGCGCATCCTTG AGACAAT	879–899	132 ^a	95°C for 10 min; 40 cycles of 95°C for 15 s; 60°C for 1 min
		TV-NSP1-qPCR-R	TTGGAGCCGGGT AGAAACAT	991–1011		
One-step RT-qPCR (binding assay)	RT-qPCR	TV-NSP1-qPCR-F	GTGCGCATCCTTG AGACAAT	879–899	132 ^a	50°C for 10 min; 95°C for 1 min, then 40 cycles of 95°C for 10 s; 60°C for 30 s
		TV-NSP1-qPCR-R	TTGGAGCCGGGT AGAAACAT	991–1011		

^aSequence of standard sample for NSP gene of Tulane virus (Integrated DNA Technologies): 5'-AGAAATTGGACCCGAATTGGCACAACACTCAG AATTGGTGTGCGCATCCTTGAGACAATAACAGGCACAATACCCCTTGGAAACCTCACCAGGAATCAATATCTGAAGTTCTGGA CGACCTCACACGGTAAAGTCCAAACAGGTGATGTTTCTACCCGGCTCCAAAGGTTGAGCGACACTATCAAAAGATCTGAGTGTGTCATG GCTTGTGATCCCTCTGCACCGCCCGAAGTTGCGC-3'(GenBank accession number: EU391643).

$$\text{Particle removal Efficiency(\%)} = \left(1 - \frac{\text{particle number concentration after placing the mask} \left(\frac{\#}{\text{cm}^3} \right)}{\text{particle number concentration before placing the mask} \left(\frac{\#}{\text{cm}^3} \right)} \right) \times 100 \quad (1)$$

The filtration efficiency tests were performed twice on each respirator after 0, 1, 3, 5, and 10 cycles of plasma exposure. The respirators were exposed to microwave only, boiling 30% hydrogen peroxide and saline only were used as the controls.

The quantitative fit testing was performed at the University of Illinois following the modified ambient aerosol condensation nuclei counter quantitative fit testing protocol (1910.134 App A, OSHA). The N95 respirators that underwent 1, 3, 5, and 10 cycles of decontamination treatment were tested.

D. CDC Filtration and Fit Testing

Masks were also sent to the National Personal Protective Technology Laboratory run by the CDC for evaluation. Eleven respirators (3 M Model 1860) that were unworn and not subjected to any pathogenic microorganisms were submitted for evaluation. This included 7 respirators that were subjected to 3 cycles of the microwave plasma decontamination process and an additional 4 respirators that served as controls. The samples were tested using a modified version of NIOSH Standard Test Procedure (STP) TEB-APR-STP-0059 to determine particulate filtration efficiency. The TSI model 8130, using sodium chloride aerosol, was used for filtration evaluation. For the laboratory fit evaluation, a static manikin headform was used to quantify changes in the manikin fit factor. The TSI PortaCount PRO+ 8038 in “N95 Enabled” mode was used for this evaluation. Additionally, tensile strength testing of the straps was performed to determine changes in strap integrity. The Instron 5943 tensile tester was used for this evaluation.

E. Plasma Spectroscopy

Spectra were obtained from the plasma in the microwave oven by drilling a hole through the back of the oven and inserting an optical fiber. The fiber was connected to an Oceanoptics HR 2000+ ER spectrometer and data between 200 and 1,100 nm were captured at various intervals during the process. The first set of decontamination experiments were conducted with a steel antenna made from a coat-hanger, but to understand the origin of the spectral lines, additional spectra were captured when using an antenna made from Cu and Al. The second and third sets of decontamination experiments were conducted with a Cu antenna.

III. RESULTS AND DISCUSSION

Tulane viruses inoculated on both sides of the respirator were reduced by a factor of $> 3\text{-log}_{10}$ ($p < 0.05$; Fig. 2). The shortest and longest distances between the plasma source

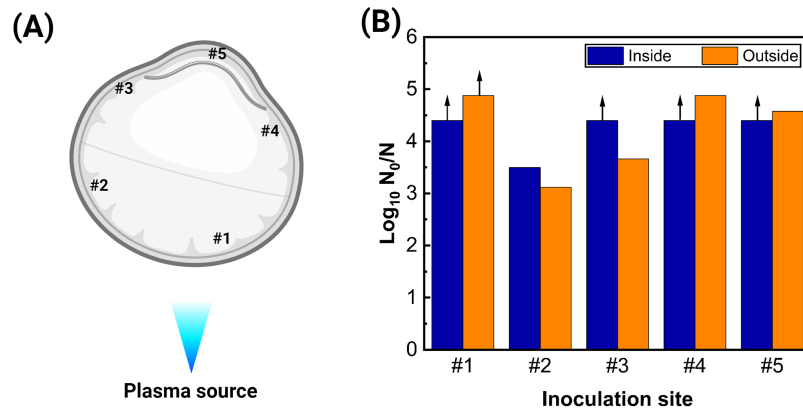


FIG. 2: Microwave-generated plasma inactivation efficacy on Tulane virus inoculated at different sites on an N95 respirator. (A) Inoculation locations of viruses on the respirator. Both inside and outside were inoculated. (B) Inactivation results after 30-seconds of plasma exposure with saline solution and 30% hydrogen peroxide. Arrows indicate points at which detection limits were reached. In these cases inactivation could be greater than shown. Infectivity loss of viruses inoculated inside and outside the respirator was significantly greater than 3-log_{10} ($p < 0.05$ by Wilcoxon Signed Rank Test, $N = 5$).

and the inoculation site were about 10 (#1) and 30 cm (#5), respectively (Fig. 2A). Although the materials for inside and outside the respirator could also affect inactivation efficacy,³⁰ in this experimental condition, there was no significant difference between infectivity loss ($p > 0.05$).

To determine the effect of each component of the decontamination unit on virus inactivation efficacy, we performed the inactivation experiments with different combinations of components (i.e., microwave, saline, 3% H₂O₂, and antenna) (Fig. 3). Note that we used commonly available concentration of hydrogen peroxide (3%) in this experiment. Although the addition of hydrogen peroxide to the microwave increased virus inactivation efficacy, neither the microwave alone nor the microwave with 3% hydrogen peroxide (i.e., no plasma) was able to achieve a reduction of more than 3-log_{10} . The temperature of the air in the microwave oven always remained below 40°C since the microwave fan was always active. This result suggested that plasma generation is essential for decontamination.

Molecular assays were conducted to examine the damage to the genome, capsid proteins, or spike proteins of the Tulane virus. Figure 4A shows the data on infectivity loss. The combination of all decontamination units showed $> 3.9\text{-log}_{10}$ infectivity reduction, but the integrity of the genome, capsid proteins, and spike proteins showed from 0.5 to 2-log_{10} reduction (red, blue, and green, respectively). There was no significant difference in integrity loss among the three viral components.

We conducted the inactivation experiments with a brown glass between the plasma source and the virus-inoculated respirator to protect the viruses from possible UV

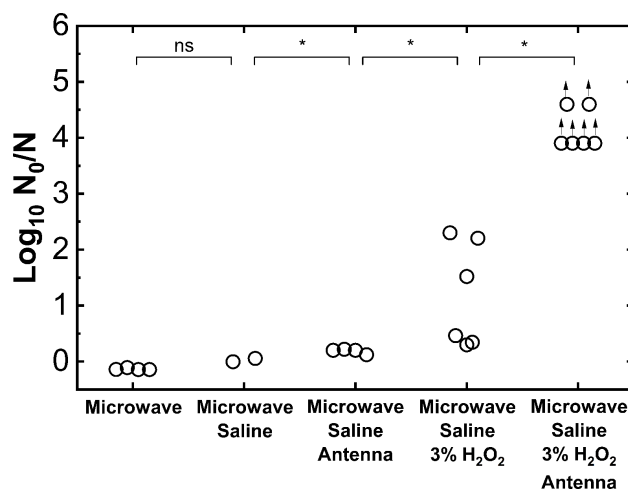


FIG. 3: Tulane virus inactivation efficacy, second set. Tick labels on *x*-axis indicate components used in decontamination treatment. In all cases the microwave was on for 40 seconds. The plasma was created when the antenna was applied (third and fifth experimental conditions). It took 10 seconds to generate the plasma, which lasted for 30 seconds. Thus, the total microwave time was still 40 seconds. Arrows indicate experiments where detection limits were reached. Inactivation could have been more effective than indicated. The Mann-Whitney Test was performed to compare two experiment conditions (ns, not significant; * $p < 0.05$).

irradiation from the plasma. We found the microwave-generated plasma did not show a significant difference in infectivity loss and damages to viral components ($p > 0.05$) with and without installation of the glass shield, and the plasma was still capable of inactivating viruses by greater than $> 3\text{-log}_{10}$. Note that we measured the UV transmittance of the brown glass with polychromatic UV irradiated by a medium-pressure Hg UV generator (Calgon Carbon Co., Pittsburgh, PA). In the range from 280 to 400 nm, the wavelength of the UV generated by plasma,³³ the UV transmittance was less than 1%. This result indicated that the glass blocked the UV irradiation caused by plasma generation.

We also conducted the same inactivation experiment with TGEV, which was used as a surrogate for the SARS-COV-2, and the results were similar to those for Tulane virus (Fig. 5). Greater than 3-log_{10} infectivity loss was achieved when all decontamination unit components were used. Even with the glass blocking UV irradiation, the microwave-generated plasma was still able to inactivate viruses by $> 3\text{-log}_{10}$.

Figure 6 shows emission spectra taken when the plasma was glowing using three materials to make the antenna. The brightest plasmas were more easily made using a copper antenna, though a bright intense plasma could be made with any material. The aluminum antenna produced the least bright plasmas and quickly melted after one or two uses. These results suggested copper as the recommended material. All of the spectra contained the Na line doublet at 589.0 and 589.6 nm and the C lines at

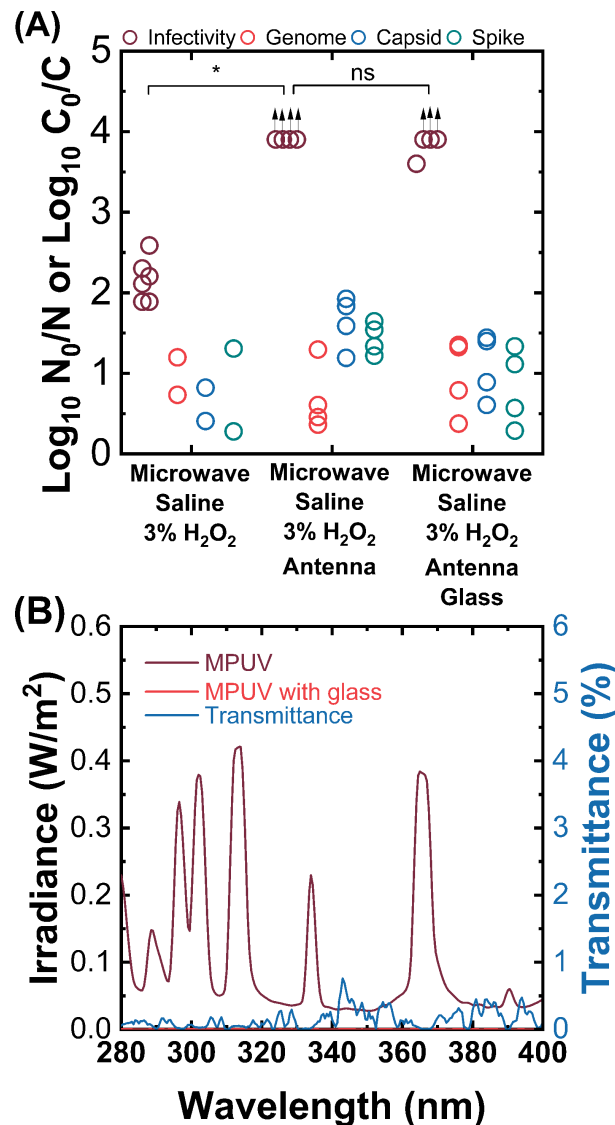


FIG. 4: Tulane virus inactivation mechanisms. (A) Infectivity of Tulane virus comparing damages on genome, capsid proteins, and spike proteins. We installed a glass shield for the third experiment, which protected the sample from plasma-generated UV radiation. Radicals could still easily flow around the shield. Arrows indicate where detection limits were exceeded. The Mann-Whitney test was performed to compare two sets of experimental conditions. Comparisons of infectivity loss are presented in the figure (ns, not significant; $*p < 0.05$). (B) UV wavelength produced by a medium-pressure UV generator was measured with the glass shield (red or straight line) and without the glass shield (dark red or wavy line). UV transmittance (blue or light wavy line) was calculated by dividing irradiance without the glass shield by irradiance with the glass shield.

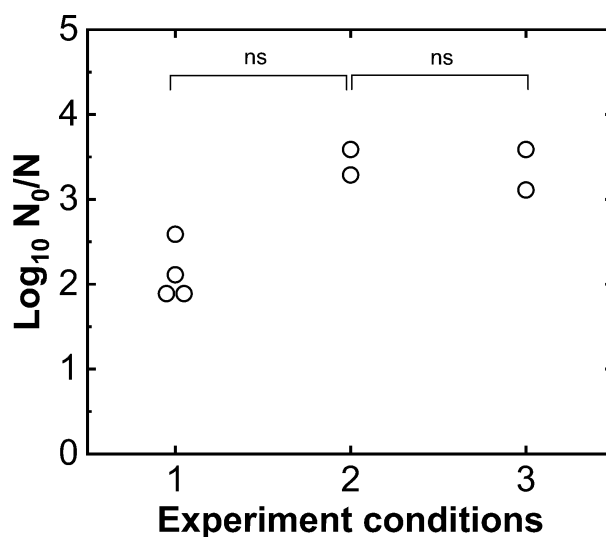


FIG. 5: TGEV inactivation efficacy in the third set of experiments. Inactivation depended on experimental conditions as discussed in the text: (1) microwave with saline and 3% hydrogen peroxide ($N=4$); (2) microwave plasma with saline, 3% hydrogen peroxide, and antenna ($N=2$), (3) conditions in item 2, with UV irradiation blocked by glass ($N=2$). The Mann-Whitney test was performed for statistical analysis between two conditions (ns, not significant).

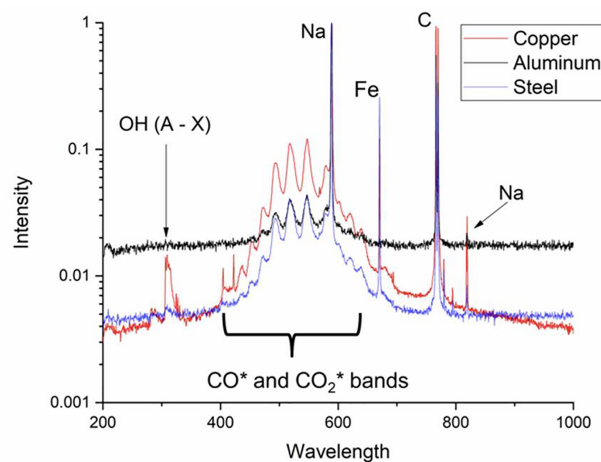


FIG. 6: Spectra of active plasma region using three antenna materials. The primary light produced is in the visible spectra as opposed to the UV. The shape of the spectra shows OH and CO radicals and CO₂ molecules in an excited state. The magnitude of the OH radical band at 300 nm is a function of the intensity of the plasma and the presence of hydrogen peroxide more so than that of the antenna material.

766.2 and 768.5 nm. The Cu and steel antenna showed an Fe line at 670.4 nm but at a lower intensity. Of most interest was the molecular vibrational and rotational bands showing the presence of excited state radicals. The OH complex around 300 nm was clearly seen in the brightest of plasmas with either the steel or the copper antenna. The continuum emission with a superimposed band structure between 400 and 650 nm was likely due to CO and CO₂ excited states.³⁴ Every plasma heated the ceramic material under the gap to the point of becoming red hot. Since this was done in air, some combustion of the carbon-containing ceramic material was expected, and that may have been the source of the carbon oxide compounds. After hundreds of exposures, a thin film of carbon soot was visible on the ceiling of the microwave, further confirming the presence of carbon in the plasma. The radicals produced by the plasma and active species appeared to be strong enough to oxidize both the genome and the proteins,^{23,24} which agreed with the molecular assay results showing molecular damages on viral genomes and proteins. Wigginton et al.³⁵ presented that singlet oxygen targets both the viral genomes and proteins. Therefore, we concluded that the radicals produced by the plasma (rather than UV) inactivated the viruses by nonspecifically targeting both genomes and proteins.

Of particular note was the lack of the 777-nm O radical emission line. Ozone is created when O radicals interact with oxygen molecules in the air. An IGS-S100 ozone meter (EP Purification) was used to monitor ozone during plasma creation. A maximum concentration of 0.16 ppm was detected in the microwave oven immediately after exposure. A concentration of 0.10 to 0.12 ppm was detected coming out of the microwave oven vent during exposure. In the background the concentration was 0.02 ppm. The levels of ozone produced in our experiment were orders of magnitude below the 120 ppm needed for sterilization quoted in Lee et al.¹⁷ Our microwave oven plasma did not generate significant amounts of ozone.

The particle filtration efficiencies of the respirator after multiple plasma exposure cycles including 30% hydrogen peroxide are shown in Fig. 7. The initial efficiencies were very similar ($\geq 99\%$). Furthermore, the tested respirators passed the fit test after 1, 3, 5, and 10 plasma exposure cycles. Collectively these results suggested that the decontamination of the N95 respirator by plasma exposure would not compromise its filtration efficiency or fit. We sent the respirators treated by 3 cycles of plasma to the CDC's NPPTP lab to analyze filtration efficiency and fit. Tables 3–5, show that there was no statistical difference between the masks undergoing 3 cycles of decontamination compared to the controls.

IV. CONCLUSION

We demonstrated how to set up a decontamination unit using available materials such as a microwave, saline, 3% H₂O₂, and a coat-hanger. We proved that microwave-generated plasma inactivates a greater than 3-log₁₀ of viral infectivity within 1 minute. From the inactivation experiments with glass shielding, plasma spectroscopy, and molecular assays, we concluded that the plasma-creating OH and other radicals (rather than UV

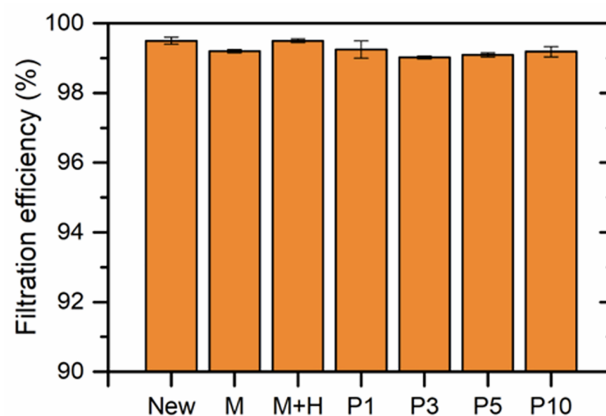


FIG 7: Filtration efficiency after plasma decontamination treatment. Filtration test results showed no statistical difference in filtration from the microwave, plasma or vapor exposures. New = clean respirator before decontamination; M and H = assumed controls after 2 minutes of microwave exposure alone and 2 minutes of microwave in with 30% hydrogen peroxide and saline, respectively. P1, P3, P5 and P10 = respirator after 1, 3, 5, and 10 plasma decontamination cycles. Error bars = standard deviation (1σ) of the duplicate measurements.

TABLE 3: Filter efficiency evaluation from CDC NPPTP

Sample	Flow rate (LPM)	Initial filter resistance (mmH ₂ O)	Initial leakage (%)	Maximum leakage (%)	Filter efficiency (%)
Three cycles of plasma-treated respirators ($N = 5$)	85	8.0 ± 0.2	0.35 ± 0.14	0.84 ± 0.25	99.2 ± 0.3
Control (no plasma treatment) ($N = 2$)	85	8.1 ± 0.1	0.29 ± 0.00	0.80 ± 0.01	99.2 ± 0.0

Note: The test method utilized in this assessment was not the NIOSH standard test procedure used for certification of respirators. Respirators assessed in this modified test do not necessarily meet the requirements of STP-0059, and therefore cannot be considered equivalent to N95 respirators tested to STP-0059.

irradiation) destroys the viral genome and proteins. The electrostatic charge in the microfibers was not investigated; however, filtration and fit were not compromised by the 10 cycles of plasma treatment.

A few notes of caution need to accompany these results. First, if possible you should dispose of contaminated masks and use new ones to ensure optimal safety. If this procedure is used to decontaminate N-95 respirators, it is important that an actual plasma is made. It is quite obvious when the system goes into continuous mode: a bright light and a loud buzzing sound are emitted by the plasma. The antenna and the material beneath

TABLE 4: Manikin fit evaluation

Sample	mFF normal breathing 1	mFF deep breathing	mFF normal breathing 2	Overall manikin fit factor
Three cycles of plasma-treated respirators ($N = 2$)	200+	200+	200+	200+
Control (no plasma treatment) ($N = 2$)	200+	200+	200+	200+

Note: Per OSHA 1910.134(f)(7), if the fit factor as determined through an OSHA-accepted quantitative fit testing protocol is equal to or greater than 100 for tight-fitting half facepieces, the fit for that respirator passes. This assessment does not include human fit testing and only uses two exercises (normal and deep breathing) on a manikin headform. It is a laboratory evaluation using a manikin headform and varies greatly from the OSHA individual fit test. Headform testing only includes normal breathing and deep breathing on a stationary (nonmoving) headform; therefore, its fit results cannot be directly translated to the standard OSHA-accepted test. Instead, this testing provides an indication of the change in fit performance (if any) associated with the decontamination of respirators.

TABLE 5: Strap integrity evaluation

Sample	Force in top strap (N)	Force in bottom strap (N)
Three cycles of plasma-treated respirators ($N = 3$)	2.93 ± 0.04	2.83 ± 0.02
Control (no plasma treatment) ($N = 2$)	2.94 ± 0.14	3.00 ± 0.12

Note: Tensile force in respirator straps was recorded at 150% strain.

the antenna gap get hot and may glow red. Thus, these surfaces should not be touched until they are cool to the touch for 5 minutes.

ACKNOWLEDGMENTS

We would like to thank Jeremy Neighbors from the Office of Occupational Safety and Health for providing the fit tests at Illinois, and Michael Bergman at the CDC's NPPTL for the fit and filtration tests performed there. Funding for this work was provided by the JUMP-ARCHES program of OSF Healthcare in conjunction with the University of Illinois.

REFERENCES

1. Zhang D, Hu M, Ji Q. Financial markets under the global pandemic of COVID-19. *Finan Res Lett*. 2020;36:101528. doi: 10.1016/j.frl.2020.101528.
2. Baker SR, Bloom N, Davis SJ, Kost K, Sammon M, Viratyosin T. The unprecedented stock market reaction to COVID-19. Review of asset pricing studies. Oxford, UK: Oxford University Press; 2020. p. 742–58.
3. Petersen E, Koopmans M, Go U, Hamer DH, Petrosillo N, Castelli F, Storgaard M, Al Khalili S, Simonsen L. Comparing SARS-CoV-2 with SARS-CoV and influenza pandemics. *Lancet Infect Dis*. 2020:e238–e44. doi: 10.1016/S1473-3099(20)30484-9.

4. Hu Z, Song C, Xu C, Jin G, Chen Y, Xu X, Ma H, Chen W, Lin Y, Zheng Y, Wang J, Hu Z, Yi Y, Shen H. Clinical characteristics of 24 asymptomatic infections with COVID-19 screened among close contacts in Nanjing, China. *Sci China Life Sci.* 2020;63(5):706–11. doi: 10.1007/s11427-020-1661-4.
5. Bai Y, Yao L, Wei T, Tian F, Jin DY, Chen L, Wang M. Presumed asymptomatic carrier transmission of COVID-19. *JAMA.* 2020;1406–7. doi: 10.1001/jama.2020.2565.
6. Brooks JT, Butler JC. Effectiveness of mask wearing to control community spread of SARS-CoV-2. *JAMA.* 2021;998–9. doi: 10.1001/jama.2021.1505.
7. Rader B, White LF, Burns MR, Chen J, Brilliant J, Cohen J, Shaman J, Brilliant L, Kraemer MUG, Hawkins JB, Scarpino SV, Astley CM, Brownstein JS. Mask-wearing and control of SARS-CoV-2 transmission in the USA: A cross-sectional study. *Lancet Digit Heal.* 2021;3(3):e148–e57. doi: 10.1016/S2589-7500(20)30293-4.
8. Aschwanden C. Five reasons why COVID herd immunity is probably impossible. *Nature.* 2021;591(7851):520–2. doi: 10.1038/d41586-021-00728-2.
9. Giordano G, Colaneri M, Di Filippo A, Blanchini F, Bolzern P, De Nicolao G, Sacchi P, Colaneri P, Bruno R. Modeling vaccination rollouts, SARS-CoV-2 variants and the requirement for non-pharmaceutical interventions in Italy. *Nat Med.* 2021;27(6):993–8. doi: 10.1038/s41591-021-01334-5.
10. Torjesen I. COVID-19: Delta variant is now UK's most dominant strain and spreading through schools. *BMJ.* 2021;373:n1445. doi: 10.1136/bmj.n1445.
11. Huang R, Huang R, Huang E. Social influences on Americans' mask-wearing behavior during COVID-19. *Int J Humanit Soc Sci.* 2021;15(5):536–44.
12. Fisher EM, Shaffer RE. Considerations for recommending extended use and limited reuse of filtering facepiece respirators in health care settings. *J Occup Environ Hyg.* 2014;11(8):37–41. doi: 10.1080/15459624.2014.902954.
13. 3M Personal Safety Division. Technical bulletin: Disinfection of filtering facepiece respirators. St Paul, MN: 3M;2020. p 3–6.
14. FDA. Recommendations for sponsors requesting EUAs for decontamination and bioburden reduction systems for surgical masks and respirators during the coronavirus disease 2019 (COVID-19) public health emergency guidance. 2020. Washington, DC: FDA.
15. Schwartz A, Stiegel M, Greeson N, Vogel A, Thomann W, Brown M, Sempowski GD, Alderman TS, Condreay JP, Burch J, Wolfe C, Smith B, Lewis S. Decontamination and reuse of N95 respirators with hydrogen peroxide vapor to address worldwide personal protective equipment shortages during the SARS-CoV-2 (COVID-19) Pandemic. *Appl Biosaf.* 2020;1–4. doi: 10.1177/1535676020919932.
16. Yang H, Hu J, Li P, Zhang C. Ultraviolet germicidal irradiation for filtering facepiece respirators disinfection to facilitate reuse during COVID-19 Pandemic: A review. *Photodiagn Photodyn Ther.* 2020;101943. doi: 10.1016/j.pdpdt.2020.101943.
17. Lee J, Bong, C, Lim W, Bae PK, Abafogi AT, Baek SH, Shin YB, Bak MS, Park S. Fast and easy disinfection of coronavirus-contaminated face masks using ozone gas produced by a dielectric barrier discharge plasma generator. *Environ Sci Technol Lett.* 2021;8(4):339–44. doi: 10.1021/acs.estlett.1c00089.
18. CDC. Decontamination and reuse of filtering facepiece respirators. 2020. Accessed 30 Sep 2021. Available from: <https://www.cdc.gov/coronavirus/2019-ncov/hcp/ppestrategy/decontaminationreuserespirators.html>.
19. Fischer RJ, Morris DH, van Doremalen N, Sarchette S, Matson MJ, Bushmaker T, Yinda CK, Seifert SN, Gamble A, Williamson BN, Judson SD, de Wit E, Lloyd-Smith JO, Munster, VJ. Effectiveness of N95 respirator decontamination and reuse against SARS-CoV-2 virus. *Emerg Infect Dis.* 2020;26(9):2253–5. doi: 10.3201/eid2609.201524.
20. Moisan M, Barbeau J, Crevier MC, Pelletier J, Philip N, Saoudi B. Plasma sterilization. Methods and mechanisms. *Pure Appl Chem.* 2002;74(3):349–58. doi: 10.1351/pac200274030349.
21. Attri P, Kim YH, Park DH, Park JH, Hong YJ, Uhm HS, Kim KN, Fridman A, Choi EH. Generation

- mechanism of hydroxyl radical species and its lifetime prediction during the plasma-initiated ultraviolet (UV) photolysis. *Sci Rep.* 2015;5(1):1–8. doi: 10.1038/srep09332.
22. Heinlin J, Isbary G, Stolz W, Morfill G, Landthaler M, Shimizu T, Steffes B, Nosenko T, Zimmermann JL, Karrer S. Plasma applications in medicine with a special focus on dermatology. *J Eur Acad Dermatol Venereol.* 2011;1–11. doi: 10.1111/j.1468-3083.2010.03702.x.
 23. Sakudo A, Yagyu Y, Onodera T. Disinfection and sterilization using plasma technology: Fundamentals and future perspectives for biological applications. *Int J Mol Sci.* 2019;216. doi: 10.3390/ijms20205216.
 24. Klämpfl TG, Isbary G, Shimizu T, Li YF, Zimmermann JL, Stolz W, Schlegel J, Morfill GE, Schmidt HU. Cold atmospheric air plasma sterilization against spores and other microorganisms of clinical interest. *Appl Environ Microbiol.* 2012;78(15):5077–82. doi: 10.1128/AEM.00583-12.
 25. Khattak HK, Bianucci P, Slepko AD. Linking plasma formation in grapes to microwave resonances of aqueous dimers. *Proc Natl Acad Sci U. S. A.* 2019;116(10):4000–5. doi: 10.1073/pnas.1818350116.
 26. Bónová L, Zhu W, Patel DK, Krogstad DV, Ruzic DN. Atmospheric pressure microwave plasma for aluminum surface cleaning. *J Vac Sci Technol A.* 2020;38(2):023002. doi: 10.1116/1.5132912.
 27. Ruzic DN. How to convert a microwave oven into a plasma-generating N-95 respirator decontamination unit. Available from: <https://youtu.be/7gm8QBbFGyM>.
 28. Araud E, Fuzawa M, Shisler JL, Li J, Nguyen TH. UV inactivation of rotavirus and Tulane virus targets different components of the virions. *Appl Environ Microbiol.* 2020;86(4):1–12. doi: 10.1128/AEM.02436-19.
 29. Araud E, Shisler JL, Nguyen TH. Inactivation mechanisms of human and animal rotaviruses by solar UVA and visible light. *Environ Sci Technol.* 2018;52(10):5682–90. doi: 10.1021/acs.est.7b06562.
 30. Oh C, Araud E, Puthussery JV, Bai H, Clark GG, Wang L, Verma V, Nguyen TH. Dry heat as a decontamination method for N95 respirator reuse. *Environ Sci Technol Lett.* 2020;7(9). doi: 10.1021/acs.estlett.0c00534.
 31. Ramm LE, Whitlow MB, Mayer MM. The relationship between channel size and the number of C9 molecules in the C5b-9 complex. *J Immunol.* 1985;134(4):2594–9.
 32. Fuzawa M, Araud E, Li J, Shisler JL, Nguyen TH. Free chlorine disinfection mechanisms of rotaviruses and human norovirus surrogate tulane virus attached to fresh produce surfaces. *Environ Sci Technol.* 2019;53(20):11999–2006. doi: 10.1021/acs.est.9b03461.
 33. Mitra A, Li YF, Klämpfl TG, Shimizu T, Jeon J, Morfill GE, Zimmermann JL. Inactivation of surface-borne microorganisms and increased germination of seed specimen by cold atmospheric plasma. *Food Bioprocess Technol.* 2014;7(3):645–53. doi: 10.1007/s11947-013-1126-4.
 34. Dobrea S, Mihaila I, Tiron V, Popa G. Optical and mass spectrometry diagnosis of a CO₂ microwave plasma discharge. *Roman Rep Physics.* 2014;66(4):1147–54.
 35. Wigginton KR, Pecson BM, Sigstam T, Bosshard F, Kohn T. Virus inactivation mechanisms: Impact of disinfectants on virus function and structural integrity. *Environ Sci Technol.* 2012;46(21):12069–78. doi: 10.1021/es3029473.